J Biol Inorg Chem (2013) 18:175–181
DOI 10.1007/s00775-012-0961-5

ORIGINAL PAPER

Why is the molybdenum-substituted tungsten-dependent formaldehyde ferredoxin oxidoreductase not active? A quantum chemical study

Rong-Zhen Liao

Received: 26 September 2012 / Accepted: 13 November 2012 / Published online: 25 November 2012

Abstract Formaldehyde ferredoxin oxidoreductase is a tungsten-dependent enzyme that catalyzes the oxidative degradation of formaldehyde to formic acid. The molybdenum ion can be incorporated into the active site to displace the tungsten ion, but is without activity. Density functional calculations have been employed to understand the incapacitation of the enzyme caused by molybdenum substitution. The calculations show that the enzyme with molybdenum (Mo-FOR) has higher redox potential than that with tungsten, which makes the formation of the Mo^{VI}=O complex endothermic by 14 kcal/mol. Following our previously suggested mechanism for this enzyme, the formaldehyde substrate oxidation was also investigated for Mo-FOR using the same quantum-mechanics-only model, except for the displacement of tungsten by molybdenum. The calculations demonstrate that formaldehyde oxidation occurs via a sequential two-step mechanism. Similarly to the tungsten-catalyzed reaction, the Mo^{VI}=O species performs the nucleophilic attack on the formaldehyde carbon, followed by proton transfer in concert with two-electron reduction of the metal center. The first step is rate-limiting, with a total barrier of 28.2 kcal/mol. The higher barrier is mainly due to the large energy penalty for the formation of the Mo^{VI}=O species.

Keywords Density functional calculations · Formaldehyde ferredoxin oxidoreductase · Tungsten · Molybdenum · Selectivity

Introduction

Molybdenum and tungsten are biologically active metals in the second and third transition metal rows of the periodic table [1–6]. They are widely distributed in the biosphere and play intimate roles in carbon, nitrogen, and sulfur metabolisms in biology [1–6]. As a result of their quite similar chemical properties, the incorporation of either metal into the active sites of several enzymes results in catalytically active species, for example, dimethyl sulfoxide reductase [7], trimethylamine *N*-oxide reductase [8], formylmethanofurane dehydrogenase [9–11], and acetylene hydratase [12]. However, some other enzymes are strictly dependent on either molybdenum or tungsten. For molybdenum-dependent sulfite oxidase and xanthine oxidase, the tungsten ion has been incorporated into the active sites of these enzymes, but leads to no activity [13]. In the case of tungsten-dependent formaldehyde ferredoxin oxidoreductase (W-FOR), the replacement of the tungsten ion by molybdenum results in the loss of activity of the enzyme (Mo-FOR) [5, 14]. The factors governing the different activities of these enzymes with tungsten or molybdenum are still less understood.

Quantum chemical methods have proven to be very powerful in the mechanistic studies of molybdenum-dependent and tungsten-dependent enzymes as well as their biomimetics [15–27]. Various insights have been obtained into the electronic structures and catalytic mechanisms of the metal complexes. The reaction mechanism of W-FOR has been investigated recently using a quantum mechanics

Electronic supplementary material The online version of this article (doi:10.1007/s00775-012-0961-5) contains supplementary material, which is available to authorized users.

R.-Z. Liao (✉)
Max-Planck-Institut für Kohlenforschung,
Kaiser-Wilhelm-Platz 1,
45470 Mülheim an der Ruhr, Germany
e-mail: rongzhen@kofo.mpg.de

(QM)-only approach [28]. On the basis of the crystal structure of the native enzyme from *Pyrococcus furiosus* [29, 30], an active-site model was devised and the B3LYP hybrid functional [31] was used to study a number of possible mechanistic scenarios. The mechanism suggested by experimentalists [29, 30] was first examined, but was found to have quite a high barrier. Then a new first-shell mechanism (see Scheme 1) was proposed for formaldehyde oxidation, in which the formaldehyde oxygen coordinates to the tungsten center directly in the Michaelis complex. A W^{VI}=O species performs a nucleophilic attack on the formaldehyde carbon, coupled with the formation of a tetrahedral intermediate, similarly to that in molybdenum-dependent aldehyde oxidoreductase (Mo-AOR) as shown by Metz et al. [19]. In the subsequent step, an anionic second-shell residue, Glu308, abstracts a proton from the tetrahedral intermediate, concomitant with a two-electron transfer from the substrate to W^{VI}, affording the reduced W^{IV} form. Both steps have quite feasible barriers, which agree quite well with experimental kinetic studies [32, 33]. To start the next catalytic cycle, the formate or formic acid product dissociates from the tungsten center, followed by the binding of a water molecule. Then the liberation of two electrons and two protons from the W^{IV}–H_2O complex (from **1** to **2**, then to **3**), using ferredoxin as an electron acceptor, generates the reactive W^{VI}=O species. On the basis of amino acid sequence comparison [34], Mo-AOR is not related to W-FOR and uses a quite different reaction mechanism. QM/molecular mechanics studies by Metz et al. [19] suggested a second-shell mechanism in which a molybdenum-bound hydroxide performs a nucleophilic attack on the aldehyde carbonyl carbon assisted by a second-shell residue, Glu869, followed by a hydride transfer to a molybdenum-bound sulfido. One of the main reasons for the two different mechanisms could be that the metals in these two enzymes have quite different ligand environments. Two pterin molecules were found bound to tungsten in W-FOR [29, 30], whereas one pterin molecule and a sulfido group were observed to coordinate to molybdenum in Mo-AOR [34].

On the basis of the catalytic cycle of W-FOR as suggested in Scheme 1, two possible scenarios can be envisaged to explain the lack of activity of Mo-FOR. The first is that the energy penalty for the formation of the Mo^{VI}=O species from the Mo^{IV}–H_2O complex increases compared with the tungsten counterpart. The second is that after molybdenum substitution, the barrier for formaldehyde oxidation by the Mo^{VI}=O species is too high for the reaction to occur. One, of course, cannot rule out other possibilities.

In the present work, the QM-only approach as adopted in our previous investigation [28] was used to unravel the factors controlling the lack of activity of Mo-FOR. The same QM-only model was used except for the substitution of molybdenum for tungsten, and the potential energy profile of the Mo^{VI}=O species formation and substrate oxidation for Mo-FOR was calculated and compared with that for W-FOR.

Computational details

The quantum chemical calculations presented herein were accomplished using the density functional B3LYP as implemented in the Gaussian 09 program package [35] Geometry optimizations were done using the 6-311+G(*d*) basis set for sulfur, the 6-31G(d,p) basis set for carbon, nitrogen, oxygen,

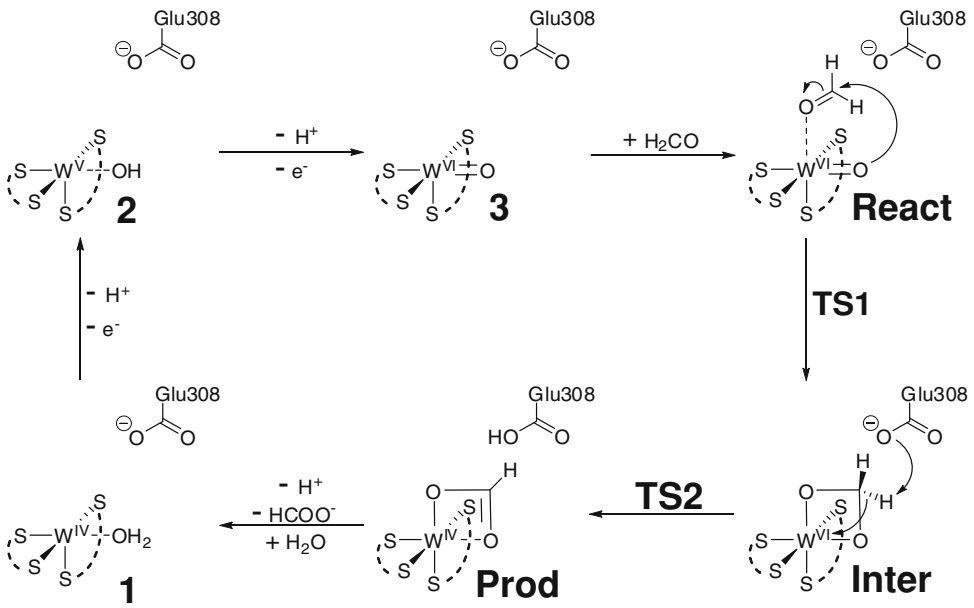

Scheme 1 Suggested reaction mechanism of formaldehyde ferredoxin oxidoreductase from calculations [9]

and hydrogen, and the LANL2TZ(f) pseudopotential [36] for tungsten and molybdenum (labeled as BS1). To obtain more accurate energies, single-point calculations on the optimized geometries were performed with the larger basis set 6-311+G(2d,2p) for carbon, nitrogen, oxygen, sulfur, and hydrogen and the LANL2TZ(f) basis set for the metals (labeled as BS2). Empirical dispersion corrections (B3LYP-D2) [37] were added, as recent studies showed that the inclusion of dispersion can significantly improve the performance of the B3LYP functional [38–41]. For comparison, further single-point calculations were also performed using the M06 functional [42] with the BS2 basis set.

The polarization effects from the protein environment were taken into account by performing single-point calculations on the optimized structures with the conductor-like polarizable continuum model [43] at the same level of theory as the geometry optimizations. The dielectric constant was set to 4, which is the value typically used in modeling the enzyme environment. Recent systematic studies on several different classes of enzymes showed that the dielectric effects of the protein environment diminish at a model size of approximately 150–200 atoms [44–47].

Analytical frequency calculations were performed at the same level of theory as the geometry optimizations in order to obtain the zero-point-energy (ZPE) effects. As will be shown later, a few key atoms at the periphery of the active-site model were kept fixed to their corresponding X-ray crystal positions during the geometry optimizations, which introduces several small imaginary frequencies, in this case on the order of 10i–40i cm^{-1}. They do not affect the ZPE obtained significantly and thus can be ignored. The B3LYP energies reported herein are with dispersion, solvation, and ZPE effects, whereas the M06 energies are with solvation and ZPE effects from B3LYP.

Active-site model

Following our previous investigation [28], a QM-only model was constructed from the crystal structure of the native enzyme (Protein Data Bank ID 1B25) [30]. The first-shell ligands of the metal (W and Mo) were represented by an oxo and two 2-methylpyranedithiolenes that mimic the pterin cofactors (Fig. 1). Truncated models of several second-shell residues—Tyr307–Glu308, Ser414–Gly415, Tyr416, and His437—were also included (Fig. 1). Hydrogen atoms were added manually. Certain atoms that are labeled with asterisks in the figures were kept fixed at their X-ray positions during the geometry optimizations to ensure the optimized structures resembled the experimental ones. The natural formaldehyde substrate was used for this study. The model is thus composed of 101 atoms and the total charge is −1.

Results and discussion

Before the investigation of formaldehyde oxidation, the energetics for the generation of the M^{VI}=O species from the M^{IV}–H_2O complex (M is W or Mo) were calculated. The redox potentials of the W(IV)/W(V) and W(V)/W(VI) couples in tungsten-dependent formaldehyde ferredoxin oxidoreductase from *Pyrococcus furiosus* have been measured to be −436 ± 20 and −365 ± 20 mV, respectively [48]. In addition, the redox potential of the electron acceptor $[Fe_4S_4]^{2+/+}$ in this enzyme has been estimated to be −350 ± 20 mV. These experimental redox potentials were used to construct the energetic profiles for the oxidation of W^{IV}–H_2O to W^{V}–OH and W^{VI}=O. The conversion of **1** to **2** for W-FOR (see Scheme 1), in which a proton and an electron are removed from the W^{IV}–H_2O complex, is exothermic by 2.0 kcal/mol, which is estimated from the redox potential differences of W(IV)/W(V) and $[Fe_4S_4]^{2+/+}$. Similarly, the transformation of **2** to **3** is also slightly exothermic, by 0.3 kcal/mol. For Mo-FOR, the redox potentials have not been reported. A practical solution to estimate the redox potentials of Mo-FOR is to calculate the relative redox potential of Mo-FOR and W-FOR. By subtracting the equations for molybdenum and tungsten as shown below, one can evaluate the relative redox potential of Mo-FOR and W-FOR with reasonable accuracy, as they have exactly the same environments before and after the oxidation/reduction [49, 50].

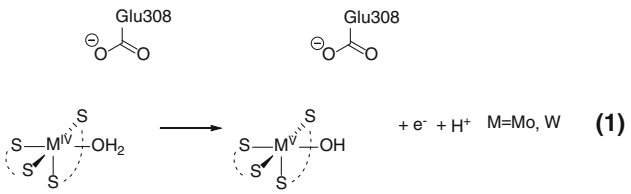

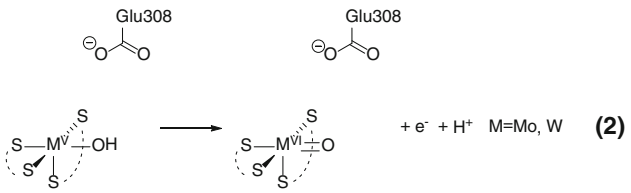

The calculations show that the oxidation of Mo^{IV} to Mo^{V} needs 8.8 (9.1) kcal/mol more than that of W^{IV} to W^{V} (energies outside and in parentheses correspond to B3LYP-D2 and M06 values, respectively), and it requires 7.5 (10.6) kcal/mol more for oxidation of Mo^{V} to Mo^{VI} than that for oxidation of W^{V} to W^{VI}. Thus, an additional energetic penalty of 16.3 (19.7) kcal/mol is present for the

formation of Mo^{VI}=O from Mo^{IV} compared with the formation of W^{VI}=O from W^{IV}. In addition, the redox potential of Mo(IV)/Mo(V) is estimated to be −55 mV using the B3LYP-D2 results, whereas it is −38 mV for the Mo(V)/Mo(VI) pair. Further experimental studies are needed to verify the present theoretical predications. The present calculations are in agreement with the experimental studies on the redox potentials of pairs of molybdenum and tungsten complexes, in which a difference of 270 mV ($E_{Mo} > E_W$, corresponding to an energy difference of 6.2 kcal/mol) was observed for complexes with sulfur ligands [51]. The redox potential difference was suggested to originate from the different bond dissociation energies (BDEs) of M^{VI}=O (M is Mo or W). The BDE difference for $MOCl_4$ (M is Mo or W) was estimated to be 26 kcal/mol ($E_{Mo} < E_W$) from an experimental study [52]. With the present active-site model, the M=O BDEs for the molybdenum and tungsten complexes are calculated to be 181.9 and 205.6 kcal/mol, respectively, indicating a difference of 23.7 kcal/mol, which is quite close to that for $MOCl_4$. These results suggest that unless a stronger oxidant with a redox potential probably higher than −38 mV appears, the Mo^{IV} center would not be oxidized to form Mo^{VI}=O.

Even though the formation of Mo^{VI}=O is highly endothermic, formaldehyde oxidation by the Mo^{VI}=O complex is also investigated, in order to understand the relative activity of Mo^{VI}=O and W^{VI}=O complexes. The binding of formaldehyde to the Mo^{VI}=O complex (from **3** to **React**) is exothermic by of 2.3 (6.6) kcal/mol, while it is almost isoenergetic for the coordination to W^{VI}=O (Fig. 2).

In the reactant complex **React** (Fig. 1), the formaldehyde oxygen is coordinated to molybdenum with a distance of 2.55 Å, which is slightly greater than that in W-FOR (2.40 Å) [28]. Similarly to the tungsten case, formaldehyde dissociates from the metal center in the triplet state. From the singlet to the triplet, one electron is excited from the dithiolene π orbital to the empty d orbital of the metal (4d for Mo and 5d for W). The metal is thus in the +5 oxidation state (W^V or Mo^V), and has an unpaired electron

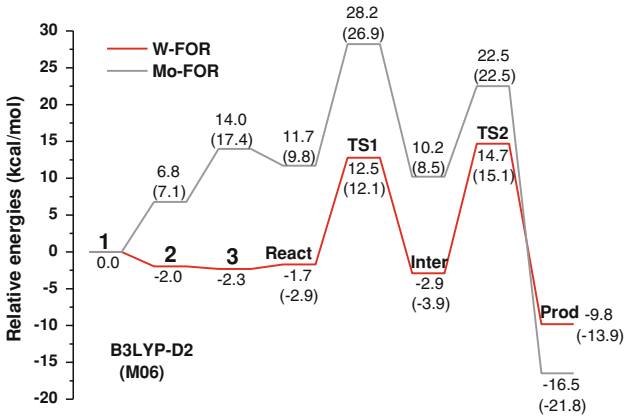

Fig. 2 Energy diagram (ΔH) for M^{VI}=O formation and formaldehyde oxidation (M is W or Mo). Values in *parentheses* are M06 energies. The energies for **2** and **3** for tungsten-dependent formaldehyde ferredoxin oxidoreductase (*W-FOR*) are taken from experimental data. Species **1** (M^{IV}) and **2** (M^V) are a triplet and a doublet, respectively; and only the singlet is shown for formaldehyde oxidation. *Mo-FOR* molybdenum-substituted W-FOR

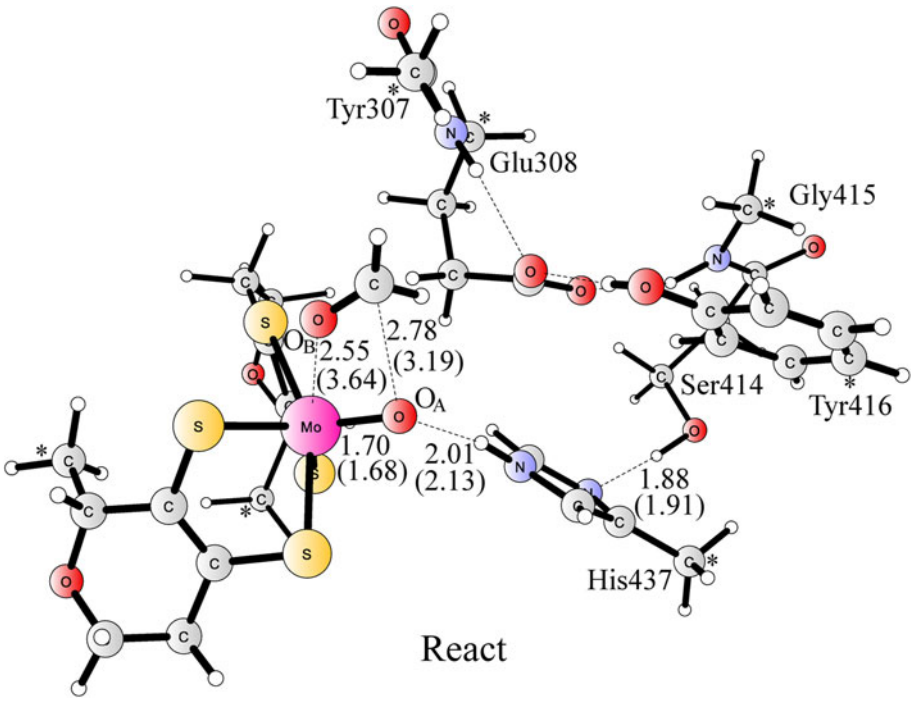

Fig. 1 Optimized reactant structure for the active site model of formaldehyde ferredoxin oxidoreductase with molybdenum substitution. Atoms with *asterisks* were fixed at their X-ray structure positions during the geometry optimizations. Distances are given in angstroms for the singlet state (distances for the triplet state are given in *parentheses*)

ferromagnetically coupled with the dithiolene radical. The singlet is the ground state, and the triplet lies at +0.8 (+6.4) kcal/mol (energies in parentheses correspond to M06 results). Similar results have been obtained for the Mo^{VI}=O model complexes of nitrate reductase [15] and dimethyl sulfoxide reductase [17]. This is quite different from the tungsten case, in which the singlet–triplet gap is much larger, being 10.2 (16.2) kcal/mol. A possible explanation is that the relativistic effect destabilizes the *d* orbitals in both molybdenum (4*d*) and tungsten (5*d*), but the effect on the latter is more significant owing to the larger mass of tunsgten [53]. The energy gap between the highest occupied molecular orbital (dithiolene π orbital) and the lowest unoccupied molecular orbital (metal *d* orbital) is thus larger in W-FOR than in Mo-FOR [54–57].

Similarly to W-FOR, we optimized all the stationary points in both the singlet and the triplet states for Mo-FOR. The structures are shown in Fig. 3 and the corresponding energies are shown in Fig. 4, where the energy of **React** is set as to be zero for better comparison of the relative activity of Mo^{VI}=O and W^{VI}=O [28]. The formaldehyde oxidation proceeds through two steps. First, Mo^{VI}=O performs a nucleophilic attack on the formaldehyde carbon via **TS1**, leading to the formation of a tetrahedral intermediate (**Inter**). The barrier is calculated to be 16.5 (17.1) kcal/mol in the singlet state and 21.3 (26.4) kcal/mol in the triplet state (Fig. 4). B3LYP and M06 thus give very similar barriers in the singlet state; however, the triplet barriers differ somewhat more significantly. **Inter** lies at −1.5 kcal/mol in the singlet state and at 1.0 kcal/mol in the triplet state. The nucleophilic attack occurs in the singlet state, with a barrier of 16.5 kcal/mol, about 2 kcal/mol higher than that for W-FOR [28] At **TS1**, the distance of the forming C–O_A bond is 1.98 Å and the Mo–O_B distance decreases to 2.22 Å (Fig. 3). These two distances are also quite similar to those in W-FOR, which are 2.02 and 2.18 Å, respectively [28]. At **Inter**, the molybdenum ion coordinates to the two negatively charged oxygens (O_A and O_B) and provides electrostatic stabilization to the intermediate.

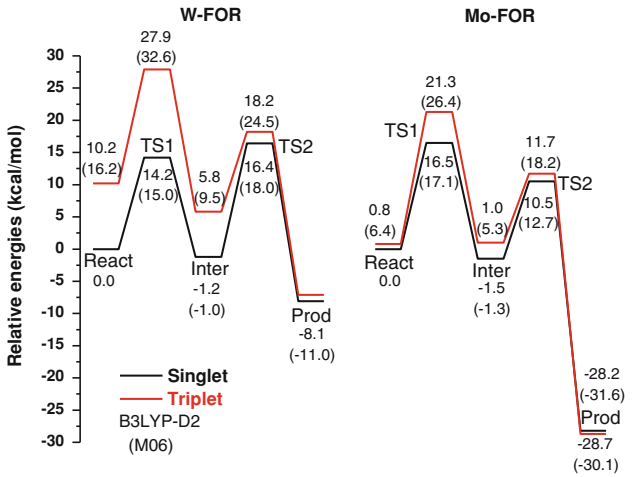

Fig. 4 Potential energy profiles (ΔH) for formaldehyde oxidation by W-FOR and Mo-FOR in the singlet and triplet states. Values in *parentheses* are M06 energies

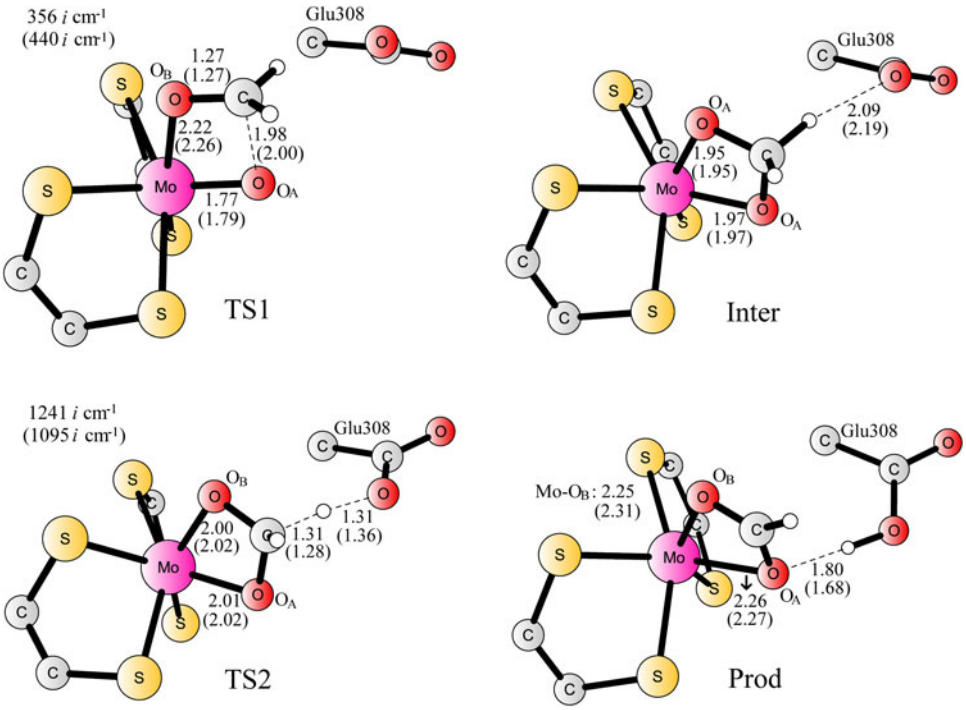

Fig. 3 Optimized geometries of stationary points for formaldehyde oxidation by Mo-FOR. For clarity, only the core of the model is shown. For the full model, see Fig. 1

The subsequent step, involving a proton transfer to Glu308, coupled with a two-electron transfer from the substrate to Mo^{VI}, has a very feasible barrier as well. The transition state (**TS2**) for this step and the leading product complex (**Prod**) were optimized and are shown in Fig. 3. The calculated energies of **TS2** are 10.5 (12.7) kcal/mol in the singlet state and 11.7 (18.2) kcal/mol in the triplet state (Fig. 4). The barriers for this step are thus about 6 kcal/mol lower than those in W-FOR (16.4 kcal/mol for the singlet at the B3LYP-D2 level) [28]. Similar results have been obtained from kinetic studies on oxo transfer reactions in the reduction of $M^{VI}O_2$ (M is W or Mo) by phosphines, in which the reduction of Mo^{VI} is faster than that of W^{VI} [58]. In addition, when the same oxo donor is used, the oxidation of W^{IV} proceeds with larger rate constants than that of Mo^{IV}, [59–62], which has also been further corroborated by density functional theory calculations on the oxo transfer reaction from dimethyl sulfoxide to $[M(OCH_3)(mdt)_2]^-$ (M is Mo or W, mdt is 1,2-dimethylethene-1,2-dithiolate(2−)) [63]. This is also in agreement with the fact that Mo^{VI}=O is a better oxidant than W^{VI}=O, and W^{IV} is easier to oxidize than Mo^{IV}. In this case, this can also be explained by the larger exothermicity for Mo-FOR than for W-FOR. As shown in Fig. 4, a difference of about 20 kcal/mol is observed. Density functional theory calculations on oxo transfer reactions of molybdenum and tungsten complexes also produce energy differences of around 20 kcal/mol, although the ligand environment is somewhat different [63–66].

Our calculations reveal that formaldehyde oxidation by the Mo^{VI}=O complex follows a two-step mechanism in the singlet, and the first step is rate-limiting, with a barrier of 16.5 (17.1) kcal/mol relative to **React**. However, considering that the formation of **React** is endothermic by as much as 11.7 (9.8) kcal/mol, the total barrier becomes 28.2 (26.9) kcal/mol. The lack of activity of Mo-FOR is thus mainly due to the energetic penalty for the formation of the active Mo^{VI}=O complex. The redox potential of the ferredoxin used for this enzyme is too low to promote the oxidation of Mo^{IV}. For W-FOR, the formation of **React** is exothermic, −1.7 (−2.9) kcal/mol, and the second step is rate-determining, with a barrier of 17.7 (19.0) kcal/mol. This is in agreement with experimental kinetic studies, where the rate constant for formaldehyde oxidation has been measured to be in the range of 4–60 s^{-1} at 80 °C [32, 33], corresponding to barriers in the range of 18–20 kcal/mol estimated using classical transition state theory.

An interesting issue is that in Mo-AOR and xanthine oxidase, a pterin cofactor and a sulfido group are seen to be bound to molybdenum [34]. The different first-shell ligand environments may help explain the use of different metals in these two enzymes.

Conclusions

In this work, density functional calculations were performed to elucidate the lack of activity in W-FOR when the tungsten ion is replaced by the molybdenum ion. The calculations demonstrate that the generation of the Mo^{VI}=O species is endothermic by 14.0 kcal/mol, owing to the use of the low-potential ferredoxin (−350 mV for this enzyme) as an electron acceptor. The redox potentials of Mo(IV)/Mo(V) and Mo(V)/Mo(VI) are estimated to be −55 and −38 mV using the experimental values for the tungsten enzyme as the reference. If the Mo^{VI}=O species can be generated, the oxidation of formaldehyde by Mo-FOR proceeds through a similar two-step mechanism in the singlet state as in W-FOR. Mo^{VI}=O acts as a nucleophile to attack the formaldehyde carbon to form a tetrahedral intermediate, followed by proton transfer coupled with two-electron reduction of Mo^{VI} to Mo^{IV}. The first step is calculated to be rate-limiting, with a barrier of 16.5 kcal/mol relative to the reactant complex. However, the total barrier becomes 28.2 kcal/mol when the energetic penalty for the formation of Mo^{VI}=O is added. The different redox potentials of these two metal complexes might be further extended to the rationalization of the different reactivity of tungsten versus molybdenum in other molybdenum/tungsten enzymes.

Acknowledgments R.-Z.L. acknowledges helpful discussions with Fahmi Himo at Stockholm University, careful revision of the manuscript by the editor, and a postdoctoral fellowship from the Max Planck Society.

References

1. Hille R (1996) Chem Rev 96:2757–2816
2. Johnson MK, Rees DC, Adams MWW (1996) Chem Rev 96:2817–2839
3. Enemark JH, Cooney JJA (2004) Chem Rev 104:1175–1200
4. Sugimoto H, Tsukube H (2008) Chem Soc Rev 37:2609–2619
5. Bevers LE, Hagedoorn PL, Hagen WR (2009) Coord Chem Rev 253:269–290
6. Romão MJ (2009) Dalton Trans 4053–4068
7. Stewart LJ, Bailey S, Bennett B, Charnock JM, Garner CD, McAlpine AS (2000) J Mol Biol 299:593–600
8. Buc J, Santini CL, Giordani R, Czjzek M, Wu LF, Giordano G (1999) Mol Microbiol 32:159–168
9. Bertram PA, Schmitz RA, Linder D, Thauer RK (1994) Arch Microbial 161:220–228
10. Bertram PA, Karrasch M, Schmitz RA, Böcher R, Albracht SPJ, Thauer RK (1994) Eur J Biochem 220:477–484
11. Vorholt JA, Vaupel M, Thauer RK (1997) Mol Microbiol 23:1033–1042
12. Boll M, Schink B, Messerschmidt A, Kroneck PMH (2005) Biol Chem 386:999–1006
13. Cohen HJ, Drew RT, Johnson JL, Rajagopalan KV (1973) Proc Natl Acad Sci USA 70:3655–3659

14. Sevcenco AM, Bevers LE, Pinkse MWH, Krijger GC, Wolterbeek HT, Verhaert PDEM, Hagen WR, Hagedoorn PL (2010) J Bacteriol 192:4143–4152
15. Leopoldini M, Russo N, Toscano M, Dulak M, Wesolowski TA (2006) Chem Eur J 12:2532–2541
16. Leopoldini M, Chiodo SG, Toscano M, Russo N (2008) Chem Eur J 14:8647–8681
17. Hofmann M (2008) Inorg Chem 47:5546–5548
18. Metz S, Thiel W (2009) J Am Chem Soc 131:14885–14902
19. Metz S, Wang D, Thiel W (2009) J Am Chem Soc 131:4628–4640
20. Vincent MA, Hillier IH, Periyasamy G, Burton NA (2010) Dalton Trans 39:3816–3822
21. Szaleniec M, Borowski T, Schühle K, Witko M, Heider J (2010) J Am Chem Soc 132:6014–6024
22. Liao RZ, Yu JG, Himo F (2010) Proc Natl Acad Sci USA 107:22523–22527
23. Liu YF, Liao RZ, Ding WJ, Yu JG, Liu RZ (2011) J Biol Inorg Chem 16:745–752
24. Liao RZ, Himo F (2011) ACS Catal 1:937–944
25. Mota CS, Rivas MG, Brondino CD, Moura I, Moura JJG, González PJ, Cerqueira NMFSA (2011) J Biol Inorg Chem 16:1255–1268
26. Metz S, Thiel W (2011) Coord Chem Rev 255:1085–1103
27. Tiberti M, Papaleo E, Russo N, De Gioia L, Zampella G (2012) Inorg Chem 51:8331–8339
28. Liao RZ, Yu JG, Himo F (2011) J Inorg Biochem 105:927–936
29. Chan MK, Mukund S, Kletzin A, Adams MWW, Rees DC (1995) Science 267:1463–1469
30. Hu Y, Faham S, Roy R, Adams MWW, Rees DC (1999) J Mol Biol 286:899–914
31. Becke AD (1993) J Chem Phys 98:5648–5652
32. Hagedoorn PL, Chen T, Schröder I, Piersma SR, de Vries S, Hagen WR (2005) J Biol Inorg Chem 10:259–269
33. Bol E, Bevers LE, Hagedoorn PL, Hagen WR (2006) J Biol Inorg Chem 11:999–1006
34. Romão MJ, Archer M, Moura I, Moura JJG, LeGall J, Engh R, Schneider M, Hof P, Huber R (1995) Science 270:1170–1176
35. Frisch MJ et al (2009) Gaussian 09, revision B.01, Gaussian, Wallingford
36. Roy LE, Hay PJ, Martin RL (2008) J Chem Theory Comput 4:1029–1031
37. Grimme S (2006) J Comput Chem 27:1787–1799
38. Lonsdale R, Harvey JN, Mulholland AJ (2010) J Phys Chem Lett 1:3232–3237
39. Siegbahn PEM, Blomberg MRA, Chen SL (2010) J Chem Theory Comput 6:2040–2044
40. Chen SL, Blomberg MRA, Siegbahn PEM (2011) J Phys Chem B 115:4066–4077
41. Santoro S, Liao RZ, Himo F (2011) J Org Chem 76:9246–9252
42. Zhao Y, Truhlar DG (2008) Theor Chem Acc 120:215–241
43. Cossi M, Gega N, Scalmani G, Barone V (2003) J Comput Chem 24:669–691
44. Sevastik R, Himo F (2007) Bioorg Chem 35:444–457
45. Hopmann KH, Himo F (2008) J Chem Theory Comput 4:1129–1137
46. Georgieva P, Himo F (2010) J Comput Chem 31:1707–1714
47. Liao RZ, Yu JG, Himo F (2011) J Chem Theory Comput 7:1494–1501
48. Koehler BP, Mukund S, Conover RC, Dhawan IK, Roy R, Adams MWW, Johnson MK (1996) J Am Chem Soc 118:12391–12405
49. Siegbahn PEM, Tye JW, Hall MB (2007) Chem Rev 107:4414–4435
50. Siegbahn PEM, Blomberg MRA (2010) Chem Rev 110:7040–7061
51. Soong SL, Chebolu V, Koch SA, O'Sullivan T, Millar M (1986) Inorg Chem 25:4067–4068
52. Holm RH, Donahue JP (1993) Polyhedron 12:571–589
53. Pyykkö P (1988) Chem Rev 88:563–594
54. Waters T, Wang XB, Yang X, Zhang L, O'Hair RAJ, Wang LS, Wedd AG (2004) J Am Chem Soc 126:5119–5129
55. Tenderholt AL, Szilagyi RK, Holm RH, Hodgson KO, Hedman B, Solomon EI (2007) J Inorg Biochem 101:1594–1600
56. Kuiper DS, Douthwaite RE, Mayol AR, Wolczanski PT, Lobkovsky EB, Cundari TR, Lam OP, Meyer K (2008) Inorg Chem 47:7139–7153
57. Majumdar A, Sarkar S (2009) Inorg Chim Acta 362:3493–3501
58. Tucci GC, Donahue JP, Holm RH (1998) Inorg Chem 37:1602–1608
59. Ueyama N, Oku H, Nakamura A (1992) J Am Chem Soc 114:7310–7311
60. Lim BS, Sung KM, Holm RH (2000) J Am Chem Soc 122:7410–7411
61. Sung KM, Holm RH (2001) J Am Chem Soc 123:1931–1943
62. Lim BS, Holm RH (2001) J Am Chem Soc 123:1920–1930
63. Tenderholt AL, Hodgson KO, Hedman B, Holm RH, Solomon EI (2012) Inorg Chem 51:3436–3442
64. McNamara JP, Hillier IH, Bhachu TS, Garner CD (2005) Dalton Trans 3572–3579
65. Lee SC, Holm RH (2008) Inorg Chim Acta 361:1166–1176
66. Hofmann M (2007) J Biol Inorg Chem 12:989–1001